

Ascending Series Analysis of the Transition Layer

S. Alzahrani¹, M. H. Hamdan^{1,*} and I. Gadoura²

¹Dept Mathematical Sciences, University of New Brunswick, Saint John, Canada

²Dept Electrical and Computer Engineering, University of New Brunswick, Canada

Abstract: This work considers existing formulation of a recent problem introduced in the literature and involves flow through a transition porous layer, whose solution has been found in terms of Airy's functions and evaluated using asymptotic series. Ascending series expressions are derived in this work and used in the computations of the solution, namely the computations of Airy's functions and the recently introduced Nield-Kuznetsov function that arises in the solution to inhomogeneous Airy's equation. Ascending series expressions developed in this work represent a viable methodology in analyzing flow through the variable permeability transition layer, and are shown to produce results as accurate as the asymptotic series results available in the literature. Both thin and fat transition layers are considered in this work which compares friction factors, velocity profiles, and mean velocities in the two types of layers, Flow through a channel over a Darcy porous layer is also considered in this work and the computed results agree with known results.

Keywords: Transition layer, airy's equation, ascending series approximations.

1. INTRODUCTION

Brinkman's equation has received considerable attention in the literature of flow through a fluid channel over a porous layer due to the compatibility of this equation with the Navier-Stokes equations. Interfacial conditions of velocity and shear stress continuity [1-4]. Served as an alternative to the Beavers and Joseph slip hypothesis [5]. However, Brinkman's equation with constant permeability and constant effective viscosity has received its share of criticism regarding its validity in describing flow through porous media [6]. Recent work, however, suggests the usefulness of Brinkman's equation with variable permeability in describing flow through a transition layer between a fluid channel and a porous medium of constant permeability porous layer the flow through which is governed by Brinkman's equation. This problem was first introduced by Nield, [7], and has been gaining popularity in the porous media literature, [8-10]. In fact, Nield and Kuznetsov, [11], have recently considered this exact problem of flow through a Brinkman layer of constant permeability bounded by a fluid layer with a transition layer sandwiched between the channel and the porous medium. Flow in the transition layer is governed by variable permeability Brinkman equation.

Nield and Kuznetsov, [11], selected a permeability distribution in the transition layer that resulted in reducing Brinkman's equation to an Airy's inhomogeneous differential equation. In their process of analysis, they introduced a new integral function that

continues to be studied due to its many useful mathematical features and potential other applications, [12]. This function has been referred to as the Nield-Kuznetsov function, and its evaluation has been through the asymptotic approximations of the Airy's functions. In fact, the results obtained in [11] have been based on asymptotic expressions of the Nield-Kuznetsov and Airy's functions. The objective of the current work is to consider the same problem introduced in [11], and to provide analysis based on ascending series approximations of the Airy's functions and the Nield-Kuznetsov function. Ascending series expressions for the Nield-Kuznetsov function are derived and use is made of the Cauchy product in its computation. Results obtained in this work are compared with those obtained by Nield and Kuznetsov [11].

2. PROBLEM FORMULATION AND SOLUTION

2.1. Problem Formulation

Following Nield and Kuznetsov, [11], flow through the three-layer configuration of thickness H , shown in Figure 1, is considered. The transition Brinkman layer is sandwiched between the fluid layer and the constant porosity porous layer, and spans the vertical dimension such that $\xi H < y^* < \eta H$.

Permeability distribution, $K = K(y^*)$, is chosen as follows.

Layer 1:

$$1/K = 0 \text{ for } 0 < y^* < \xi H. \quad (1a)$$

*Address correspondence to this author at the Dept Mathematical Sciences, University of New Brunswick, Saint John, Canada; Tel: 1-506-648-5625; E-mail: hamdan@unb.ca

Layer 2:

$$\frac{1}{K} = \frac{y^* - \xi H}{K_0(\eta - \xi)H} \text{ for } \xi H < y^* < \eta H. \quad (1b)$$

Layer 3:

$$K = K_0 \text{ for } \eta H < y^* < H, \quad (1c)$$

where K_0 is a constant permeability.

Assuming there is a uniform and common constant negative pressure gradient $G = -P_x$ throughout the domain and that the Brinkman model is employed in each porous layer and Navier-Stokes equations in the fluid layer, the equations governing the flow in the three layers are as follows:

$$\mu \frac{d^2 u_1^*}{dy^{*2}} + G = 0; 0 < y^* < \xi H, \quad (2a)$$

$$\mu_{e2} \frac{d^2 u_2^*}{dy^{*2}} - \frac{\mu}{K_2} u_2^* + G = 0; \xi H < y^* < \eta H, \quad (2b)$$

and

$$\mu_{e3} \frac{d^2 u_3^*}{dy^{*2}} - \frac{\mu}{K_3} u_3^* + G = 0; \eta H < y^* < H, \quad (2c)$$

where in μ is the base fluid viscosity, μ_{e2} and μ_{e3} are effective viscosities of the fluid in layers 2 and 3, respectively, and u_1^* , u_2^* , and u_3^* are the tangential velocity components in layers 1, 2 and 3, respectively.

Introducing the dimensionless variables $y = \frac{y^*}{H}$,

$$u = \frac{\mu u^*}{GH^2}, \text{ and defining the Darcy number as}$$

$$Da = \frac{K_0}{H^2} Da, \text{ and denoting the viscosity ratios } M_2$$

$$\text{and } M_3 \text{ by } M_2 = \frac{\mu_{e2}}{\mu}, M_3 = \frac{\mu_{e3}}{\mu}, \text{ governing equations}$$

2(a, b, c), take the following forms respectively:

$$\frac{d^2 u_1}{dy^2} + 1 = 0; 0 < y < \xi, \quad (3a)$$

$$M_2 \frac{d^2 u_2}{dy^2} - \frac{1}{Da} \left(\frac{y - \xi}{\eta - \xi} \right) u_2 + 1 = 0 \text{ for } \xi < y < \eta, \quad (3b)$$

and

$$M_3 \frac{d^2 u_3}{dy^2} - \frac{u_3}{Da} + 1 = 0; \eta < y < 1. \quad (3c)$$

Equations 3(a, b, c) are to be solved subject to no-slip boundary conditions on solid walls ($y=0$ and $y=1$), and the matching conditions of velocity and shear stress continuity at the interfaces ($y=\xi$ and $y=\eta$) between layers, namely;

$$u_1 = 0 \text{ at } y = 0, \quad (4a)$$

$$u_3 = 0 \text{ at } y = 1, \quad (4b)$$

$$u_1 = u_2 \text{ at } y = \xi, \quad (4c)$$

$$u_2 = u_3 \text{ at } y = \eta, \quad (4d)$$

$$\frac{du_1}{dy} = \frac{du_2}{dy} \text{ at } y = \xi, \quad (4e)$$

and

$$\frac{du_2}{dy} = \frac{du_3}{dy} \text{ at } y = \eta. \quad (4f)$$

Now, defining;

$$\lambda_2 = \frac{1}{[M_2 Da (\eta - \xi)]^{1/3}}, \quad (5)$$

$$\lambda_3 = \frac{1}{(M_3 Da)^{1/2}}, \quad (6)$$

$$\tilde{y} = \lambda_2 (y - \xi), \quad (7)$$

and writing;

$$u_2(y) \equiv U_2(\tilde{y}), \quad (8)$$

equations (3a), (3b), and (3c) are re-written as;

$$\frac{d^2 u_1}{dy^2} + 1 = 0; 0 < y < \xi, \quad (9a)$$

$$\frac{d^2 U_2}{d\tilde{y}^2} - \tilde{y} U_2 + \frac{1}{M_2 \lambda_2^2} = 0 \text{ for;}$$

$$0 < \tilde{y} < \lambda_2 (\eta - \xi), \quad (9b)$$

and

$$\frac{d^2 u_3}{dy^2} - \lambda_3^2 u_3 + \frac{1}{M_3} = 0; \eta < y < 1. \quad (9c)$$

2.2. Velocity Expressions

Equations (9a) and (9c) possess the following general solutions, respectively;

$$u_1 = \frac{-y^2}{2} + c_1 y + d_1, \tag{10}$$

$$u_3 = c_3 \exp(\lambda_3 y) + d_3 \exp(-\lambda_3 y) + \frac{1}{M_3 \lambda_3^2}. \tag{11}$$

Equation (9b) is recognized as Airy; s inhomogeneous differential equation. The homogeneous part of (9b) possesses the complementary solution

$$U_2 = c_2 A_i(\tilde{y}) + d_2 B_i(\tilde{y}), \tag{12}$$

where $A_i(\tilde{y})$ and $B_i(\tilde{y})$ are Airy's functions of the first and second kind, respectively [12].

The Wronskian of $A_i(y)$ and $B_i(y)$ is given by:

$$A_i(\tilde{y}) B_i'(\tilde{y}) - B_i(\tilde{y}) A_i'(\tilde{y}) = 1 / \pi \tag{13}$$

and the particular solution of (9b) is obtained by the method of Variation of Parameters as;

$$U_p = \frac{\pi}{M_2 \lambda_2^2} N_i(\tilde{y}), \tag{14}$$

where;

$$N_i(\tilde{y}) = A_i(\tilde{y}) \int_0^{\tilde{y}} B_i(t) dt - B_i(\tilde{y}) \int_0^{\tilde{y}} A_i(t) dt \tag{15}$$

is the Nield-Kuznetsov function whose derivative is given by

$$N_i'(\tilde{y}) = A_i'(\tilde{y}) \int_0^{\tilde{y}} B_i(t) dt - B_i'(\tilde{y}) \int_0^{\tilde{y}} A_i(t) dt \tag{16}$$

and the values at zero are $N_i(0) = N_i'(0) = 0$.

The general solution to equation (9b) is expressed with the help of (8) as:

$$u_2(y) = U_2(\tilde{y}) = c_2 A_i(\tilde{y}) + d_2 B_i(\tilde{y}) + \frac{\pi}{M_2 \lambda_2^2} N_i(\tilde{y}) \tag{17}$$

Using (7) in (17), the following equation is obtained:

$$u_2 = c_2 A_i(\lambda_2(y - \xi)) + d_2 B_i(\lambda_2(y - \xi)) + \frac{\pi}{M_2 \lambda_2^2} N_i(\lambda_2(y - \xi)) \tag{18}$$

2.3. Shear Stress Expressions

Shear stress terms across the layers are obtained from equations (10), (11) and (18), respectively, and take the following forms:

$$u_1'(y) = -y + c_1, \tag{19}$$

$$u_3'(y) = c_3 \lambda_3 \exp(\lambda_3 y) - d_3 \lambda_3 \exp(-\lambda_3 y), \tag{20}$$

and

$$u_2'(y) = c_2 \lambda_2 A_i'(\lambda_2(y - \xi)) + d_2 \lambda_2 B_i'(\lambda_2(y - \xi)) + \frac{\pi}{M_2 \lambda_2^2} \lambda_2 N_i'(\lambda_2(y - \xi)), \tag{21}$$

where "prime" notation denotes differentiation with respect to the argument.

2.4. Mean Velocity Expressions

A measure of the overall volume flux through the channel is the dimensionless mean velocity \bar{u} defined by;

$$\bar{u} = \int_0^{\xi} u_1 dy + \int_{\xi}^{\eta} u_2 dy + \int_{\eta}^1 u_3 dy. \tag{22}$$

Using equations (10), (11) and (18) in (22) results in:

$$\begin{aligned} \bar{u} = & \frac{1}{2} c_1 \xi^2 + d_1 \xi - \frac{1}{6} \xi^3 + \frac{c_2}{\lambda_2} \int_0^{\lambda_2(\eta - \xi)} A_i(t) dt \\ & + \frac{d_2}{\lambda_2} \int_0^{\lambda_2(\eta - \xi)} B_i(t) dt + \frac{\pi}{M_2 \lambda_2^2} \int_0^{\lambda_2(\eta - \xi)} N_i(t) dt \\ & + \frac{c_3}{\lambda_3} (\exp(\lambda_3) - \exp(\lambda_3 \eta)) \\ & - \frac{d_3}{\lambda_3} (\exp(-\lambda_3) - \exp(-\lambda_3 \eta)) + \frac{1 - \eta}{M_3 \lambda_3^2} \end{aligned} \tag{23}$$

2.5. Friction Factor Expression

A further quantity of interest is the value of the friction factor, c_f , define as $-du_1 / dy$ at $y = \xi$. This represents the dimensionless frictional stress in the fluid at the interface between the fluid and the porous medium, and takes the form;

$$c_f = \xi - c_1. \tag{24}$$

2.6. Matrix Expression for the Arbitrary Constants

In order to determine the arbitrary constants in equations (10), (11) and (18), conditions 4(a-f) used, and the resulting linear equations are cast in the following matrix-vector form:

$$M\bar{x} = \bar{c} \tag{25}$$

where M is the coefficient matrix given by;

$$\begin{matrix} 0 & 1 & 0 & 0 & 0 & 0 \\ \xi & 1 & -A_i(0) & -B_i(0) & 0 & 0 \\ 1 & 0 & -\lambda_2 A_i'(0) & -\lambda_2 B_i'(0) & 0 & 0 \\ 0 & 0 & A_i \lambda_2 (\eta - \xi) & B_i \lambda_2 (\eta - \xi) & -e^{\lambda_3 \eta} & -e^{-\lambda_3 \eta} \\ 0 & 0 & \lambda_2 A_i' \lambda_2 (\eta - \xi) & \lambda_2 B_i' \lambda_2 (\eta - \xi) & -\lambda_3 e^{\lambda_3 \eta} & \lambda_3 e^{-\lambda_3 \eta} \\ 0 & 0 & 0 & 0 & e^{\lambda_3} & e^{-\lambda_3} \end{matrix} \tag{26}$$

$$\bar{x} = \begin{bmatrix} c_1 \\ d_1 \\ c_2 \\ d_2 \\ c_3 \\ d_3 \end{bmatrix} \tag{27}$$

and

$$\bar{c} = \begin{bmatrix} 0 \\ \xi^2 / 2 \\ \xi + \frac{\pi}{M_2 \lambda_2} N_i'(0) \\ \frac{1}{M_3 \lambda_3^2} - \frac{\pi}{M_2 \lambda_2} N_i[\lambda_2 (\eta - \xi)] \\ -\frac{\pi}{M_2 \lambda_2} N_i'[\lambda_2 (\eta - \xi)] \\ -1 / M_3 \lambda_3^2 \end{bmatrix}. \tag{28}$$

2.7. Computation and Evaluation of Special Functions

Determining the arbitrary constants in (25), and evaluation of solution (18), necessitates evaluating Airy's functions and the Nield-Kuznetsov function, [12]. Two popular methods of evaluation are the asymptotic series and the ascending series methods. In their analysis, Nield and Kuznetsov, [11], used asymptotic

series, valid for large arguments, to evaluate the said functions. In the current work, solutions are expressed in terms of the following ascending series.

Letting $a_1 = A_i(0) \approx 0.3550280538878172$ and $a_2 = -A_i'(0) \approx 0.2588194037928067$, and letting $(b)_k$ be the Pochhammer symbol, [12], given by:

$$(b)_k = \frac{\Gamma(b+k)}{\Gamma(b)}, \tag{29}$$

$$= b(b+1)(b+2)...(b+k-1); k > 0$$

with $(b)_0 = 1$, Airy's functions, their derivatives and integrals can be expressed as:

$$A_i(x) = a_1 \sum_{k=0}^{\infty} \left(\frac{1}{3}\right)_k \frac{3^k x^{3k}}{(3k)!} - a_2 \sum_{k=0}^{\infty} \left(\frac{2}{3}\right)_k \frac{3^k x^{3k+1}}{(3k+1)!} \tag{30}$$

$$A_i'(x) = a_1 \sum_{k=0}^{\infty} \left(\frac{1}{3}\right)_k \frac{3^k x^{3k-1}}{(3k-1)!} - a_2 \sum_{k=0}^{\infty} \left(\frac{2}{3}\right)_k \frac{3^k x^{3k}}{(3k)!} \tag{31}$$

$$\int_0^x A_i(t) dt = a_1 \sum_{k=0}^{\infty} \left(\frac{1}{3}\right)_k \frac{3^k x^{3k+1}}{(3k+1)!} - a_2 \sum_{k=0}^{\infty} \left(\frac{2}{3}\right)_k \frac{3^k x^{3k+2}}{(3k+2)!} \tag{32}$$

$$B_i(x) = \sqrt{3} a_1 \sum_{k=0}^{\infty} \left(\frac{1}{3}\right)_k \frac{3^k x^{3k}}{(3k)!} + \sqrt{3} a_2 \sum_{k=0}^{\infty} \left(\frac{2}{3}\right)_k \frac{3^k x^{3k+1}}{(3k+1)!} \tag{33}$$

$$B_i'(x) = \sqrt{3} a_1 \sum_{k=0}^{\infty} \left(\frac{1}{3}\right)_k \frac{3^k x^{3k-1}}{(3k-1)!} + \sqrt{3} a_2 \sum_{k=0}^{\infty} \left(\frac{2}{3}\right)_k \frac{3^k x^{3k}}{(3k)!} \tag{34}$$

$$\int_0^x B_i(t) dt = \sqrt{3} a_1 \sum_{k=0}^{\infty} \left(\frac{1}{3}\right)_k \frac{3^k x^{3k+1}}{(3k+1)!} + \sqrt{3} a_2 \sum_{k=0}^{\infty} \left(\frac{2}{3}\right)_k \frac{3^k x^{3k+2}}{(3k+2)!} \tag{35}$$

Using definitions (15) and (16), and making use of (29) to (35), the following expressions for $N_i(x)$ and $N_i'(x)$ are obtained, respectively:

$$N_i(x) = 2\sqrt{3}a_1a_2 \begin{bmatrix} \left\{ \sum_{k=0}^{\infty} \left(\frac{1}{3}\right)_k \frac{3^k x^{3k}}{(3k)!} \right\} \\ \left\{ \sum_{k=0}^{\infty} \left(\frac{2}{3}\right)_k \frac{3^k x^{3k+2}}{(3k+2)!} \right\} \\ - \left\{ \sum_{k=0}^{\infty} \left(\frac{2}{3}\right)_k \frac{3^k x^{3k+1}}{(3k+1)!} \right\} \\ \left\{ \sum_{k=0}^{\infty} \left(\frac{1}{3}\right)_k \frac{3^k x^{3k+1}}{(3k+1)!} \right\} \end{bmatrix} \quad (36)$$

$$N'_i(x) = 2\sqrt{3}a_1a_2 \begin{bmatrix} \left\{ \sum_{k=0}^{\infty} \left(\frac{1}{3}\right)_k \frac{3^k x^{3k-1}}{(3k-1)!} \right\} \\ \left\{ \sum_{k=0}^{\infty} \left(\frac{2}{3}\right)_k \frac{3^k x^{3k+2}}{(3k+2)!} \right\} \\ - \left\{ \sum_{k=0}^{\infty} \left(\frac{2}{3}\right)_k \frac{3^k x^{3k}}{(3k)!} \right\} \\ \left\{ \sum_{k=0}^{\infty} \left(\frac{1}{3}\right)_k \frac{3^k x^{3k+1}}{(3k+1)!} \right\} \end{bmatrix} \cdot \quad (37)$$

In order to evaluate expressions (36) and (37), and to find $\int_0^x N_i(t)dt$, use is made of the Cauchy product to express (36) and (37), respectively as;

$$N_i(x) = 2\sqrt{3}a_1a_2 \sum_{k=0}^{\infty} 3^k \left(\sum_{l=0}^k \left(\frac{1}{3}\right)_l \left(\frac{2}{3}\right)_{k-l}^* \frac{-3k+6l-1}{(3l+1)!(3(k-l)+2)!} \right) x^{3k+2} \quad (38)$$

and

$$N'_i(x) = 2\sqrt{3}a_1a_2 \sum_{k=0}^{\infty} 3^k (3k+2) \left(\sum_{l=0}^k \left(\frac{1}{3}\right)_l \left(\frac{2}{3}\right)_{k-l}^* \frac{-3k+6l-1}{(3l+1)!(3(k-l)+2)!} \right) x^{3k+1} \quad (39)$$

and from (38), the following integral is obtained:

$$\int_0^x N_i(t)dt = 2\sqrt{3}a_1a_2 \sum_{k=0}^{\infty} 3^k \left(\sum_{l=0}^k \left(\frac{1}{3}\right)_l \left(\frac{2}{3}\right)_{k-l}^* \frac{-3k+6l-1}{(3l+1)!(3(k-l)+2)!} \right) \frac{x^{3k+3}}{3k+3} \quad (40)$$

2.8. Computational Algorithm

Computations to render the stated problem completely solved proceed according to the following algorithm:

1. Select Darcy number, Da , and the boundaries of the transition layer, $y = \xi$ and $y = \eta$.
2. Select viscosity ratio M_2 and M_3 .
3. Calculate λ_2 and λ_3 using equations (5) and (6), respectively.
4. Using the ascending series expressions, derived above, calculate entries in the coefficient matrix (26) and the right-hand-side vector (28).
5. Using *Maple*, solve the matrix equation (25) for the arbitrary constants appearing in equations equations (10), (11) and (18). With the values of the arbitrary constants known, the velocity profiles (10), (11) and (18) are completely determined.
6. Calculate the shear stress in each layer given in equations (19), (20) and (21).
7. Calculate the mean velocity in equation (23) and the friction factor in equation (24).

3. TWO-LAYER, DARCY FLOW MODEL WITH BEAVERS-JOSEPH CONDITION

For the sake of comparison, the current work also considers the second situation treated by Nield and Kuznetsov [11], namely where a Darcy-type porous layer terminates a clear fluid channel and the Beavers–Joseph boundary condition [5] is imposed at the interface between layers. The governing equations are:

In the clear fluid channel;

$$\frac{d^2 u_{D1}}{dy^2} + 1 = 0; \quad 0 < y < \xi \quad (41)$$

In the Darcy layer;

$$-\frac{u_{D2}}{Da} + 1 = 0; \quad \xi < y < 1 \quad (42)$$

Boundary and matching conditions are:

$$u_{D1} = 0 \text{ at } y = 0, \quad (43)$$

$$\frac{du_{D1}}{dy} = -\beta(u_{D1} - u_{D2}) \text{ at } y = \xi, \quad (44)$$

where $\beta = \frac{\alpha}{\sqrt{Da}}$ and α is the Beavers–Joseph slip parameter.

The velocity distribution in the channel is the solution to (41) satisfying the given boundary conditions, and takes the form;

$$u_{D1} = \frac{\xi + \frac{1}{2}\beta\xi^2 + \beta Da}{(1 + \beta\xi)} y - \frac{1}{2}y^2 \quad (45)$$

and the Darcy velocity in the porous layer is the uniform velocity;

$$u_{D2} = Da. \quad (46)$$

The mean velocity across the two layers is given by;

$$\bar{u}_D = \int_0^\xi u_{D1} dy + \int_\xi^1 u_{D2} dy = \int_0^\xi \left(\frac{\xi + \frac{1}{2}\beta\xi^2 + \beta Da}{(1 + \beta\xi)} y - \frac{1}{2}y^2 \right) dy + \int_\xi^1 Da dy \quad (47)$$

or

$$\bar{u}_D = \frac{1}{12(1 + \beta\xi)} [4\xi^3 + \beta\xi^4 + (12 - 12\xi + 12\beta\xi - 6\beta\xi^2)Da] \quad (48)$$

and the friction coefficient is given by;

$$c_{fD} = -\frac{du_{D1}}{dy} \Big|_{y=\xi} = \frac{\beta\xi^2 - 2\beta Da}{2(1 + \beta\xi)}. \quad (49)$$

4. RESULTS AND DISCUSSION

For the flow in the triple layer, Figure 1, Results have been obtained for the range of Darcy number, $Da = 1.0$, $Da = 0.1$, $Da = 0.01$, $Da = 0.0006$, $Da = 0.0005$ and $Da = 0.0004$. The value of $Da = 0.0004$ is the lowest value used, while computed results are accurate using *Maple*. Nield and Kuznetsov, [11], reported results for Da as low as 0.0002 using *Mathematica*. Computations were carried out for thin transition layer ($\xi = 0.49$ and $\eta = 0.51$) and fat (thick) transition layer ($\xi = 1/3$ and $\eta = 2/3$).

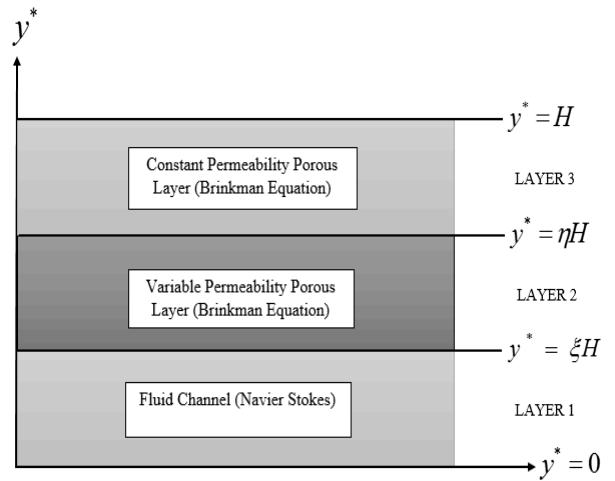


Figure 1: Representative Sketch.

In the absence of accurate values for the effective viscosity, viscosity ratios have been chosen as $M_2 = M_3 = 1$. However, for the flow in the channel bounded by Darcy layer, we use $Da = 0.0002$.

Values of the arbitrary constants appearing in equations (10), (11) and (18), and computed through the matrix-vector equation (25), are listed in Table 1 for different values of Da and the two transition layer thicknesses employed. The arbitrary constants were computed using 16 digits and used in their full accuracy in the computation of velocity profiles, mean velocities, and friction factors. However, in Table 1(a, b), we list 5 decimal places of accuracy.

Table 1(a): Values of $c_1, d_1, c_2, d_2, c_3, d_3$, for Different Darcy Number and Layer Thicknesses

Da		Da = 1	Da = 0.1
$\xi = 1/3$ $\eta = 2/3$	c_1	0.48715	0.41311
	d_1	0	0
	c_2	-0.05558	0.06609
	d_2	0.20582	0.09543
	c_3	-0.27103	-0.00428
	d_3	-0.71560	0.02997
$\xi = 0.49$ $\eta = 0.51$	c_1	0.48771	0.41841
	d_1	0	0
	c_2	0.16869	0.137099
	d_2	0.09601	0.05903
	c_3	-0.27095	-0.00428
	d_3	-0.71625	0.02434

Table 1(b): Values of $c_1, d_1, c_2, d_2, c_3, d_3$, for Different Darcy Number and Layer Thicknesses

Da		Da = 0.01	Da = 0.0006
$\xi = 1/3$ $\eta = 2/3$	c_1	0.28391	0.20965
	d_1	0	0
	c_2	0.06930	0.03415
	d_2	0.02354	0.00358
	c_3	-4.5988×10^{-7}	-1.1172×10^{-21}
	d_3	2.8554	1.6951×10^7
$\xi = 0.49$ $\eta = 0.51$	c_1	0.30797	0.26223
	d_1	0	0
	c_2	0.06402	0.02196
	d_2	0.01322	0.00105
	c_3	-4.5985×10^{-7}	-1.1172×10^{-21}
	d_3	2.8353	4.1707×10^6

Values of the mean velocity across the three-layered configuration, \bar{u} , together with the friction factor c_f , and the mean velocity across the channel bounded by Darcy layer, \bar{u}_D , together with the associated friction factor, c_{fD} , are listed in Table 2(a, b).

Table 2(a): Values of Mean Velocity \bar{u} and Friction Coefficient c_f for Various Da, for Fat and Thin Transition Layers

	Da = 1		Da = 0.1	
	Fat	Thin	Fat	Thin
\bar{u}	0.0794 0.0794*	0.0794 0.0794*	0.0569	0.0574
\bar{u}_D	0.7184 0.6145	0.6201 0.6146*	0.0828	0.0872
c_f	-0.1538 -0.153*	0.0023 0.002*	-0.0798	0.0716
c_{fD}	-0.7082 -0.583*	-0.5906 -0.583*	-0.0684	0.0249

* Nield and Kuznetsov Results, [11].

In the Darcy configuration, we used $\alpha = 1$, chosen as a representative value. Values computed in this work are compared with those reported in [11]. Table 2 shows that there is exact agreement in the values of \bar{u} and c_f (up to within the number of significant digits reported) between the current computations that use

ascending series representations, and Nield and Kuznetsov's results, obtained using asymptotic series approximations, [11]. For the values of \bar{u}_D and c_{fD} ,

Table 2 shows a slight discrepancy between the current results and those obtained in [11], (even though current computations are based on their solutions for the Darcy case). The behavior of \bar{u}_D and c_{fD} computed here is a mirror image of the corresponding behavior they reported. This behavior is illustrated in Figure 2 and 3, below, produced when $Da = 0.0002$. Figure 2 shows the decrease of the mean velocity, \bar{u}_D , with increasing α (along a curve that resembles a rectangular hyperbola), while Figure 3 shows a sharp and rapid increase in c_{fD} with a slight increase in α . The c_{fD} curve flattens with further increase in α .

Table 2(b): Values of Mean Velocity \bar{u} and Friction Coefficient c_f for Various Da, for Fat and Thin Transition Layers

	Da = 0.01		Da = 0.0006	
	Fat	Thin	Fat	Thin
\bar{u}	0.0207 0.0207*	0.0236 0.0236*	0.0068	0.0142
\bar{u}_D	0.0132 0.0227*	0.0219 0.0227*	0.0042	0.0117
c_f	0.0494 0.049*	0.1820 0.182*	0.1237	0.2278
c_{fD}	0.1051 0.192*	0.1865 0.192*	0.1536	0.2322

* Nield and Kuznetsov Results, [11].

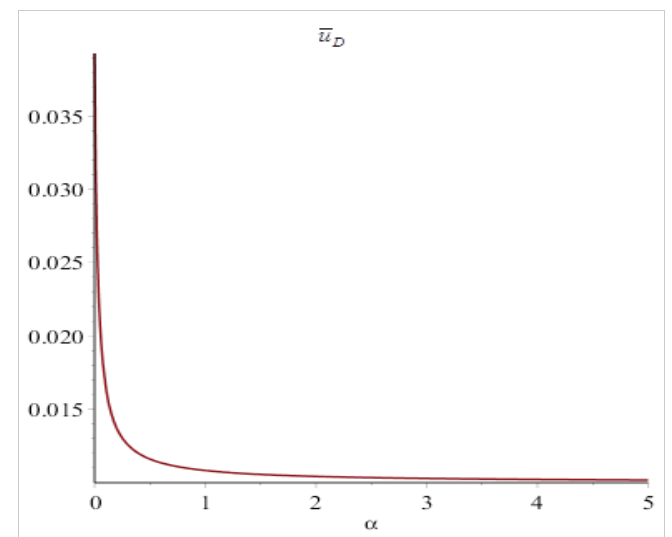


Figure 2: Mean velocity \bar{u}_D as a function of the slip parameter α . $Da=0.0002$.

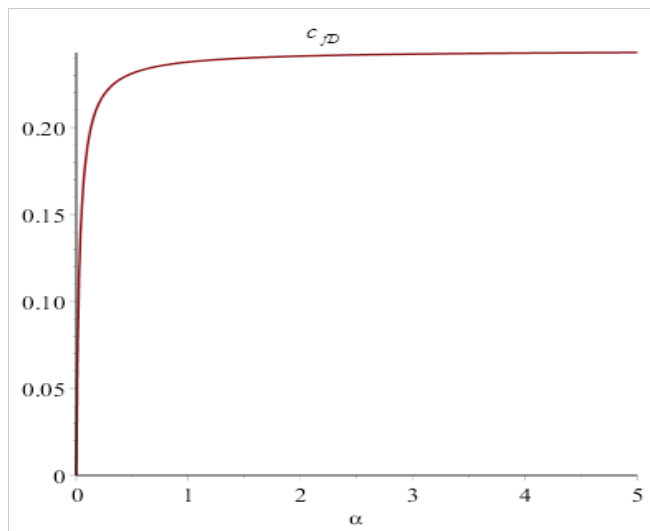


Figure 3: Friction factor c_{fD} as a function of the slip parameter α . $Da=0.0002$.

Velocity profiles in the channel sandwiching the transition layer are shown in Figures 4 to 9 to illustrate the effects of the transition layer thickness and the effects of Darcy number. For the case of $Da = 1$, Figure 4 shows that the profile across the channel is not affected by the transition layer thickness. For both thin and fat layers, the velocity profiles are the same (graphically) and are parabolic-like. This is an expected behavior since for $Da = 1$, the permeability approaches infinity and flow in the three-layered channel resembles the Navier-Stokes' Poiseuille flow. This is in agreement with the profiles reported in [11].

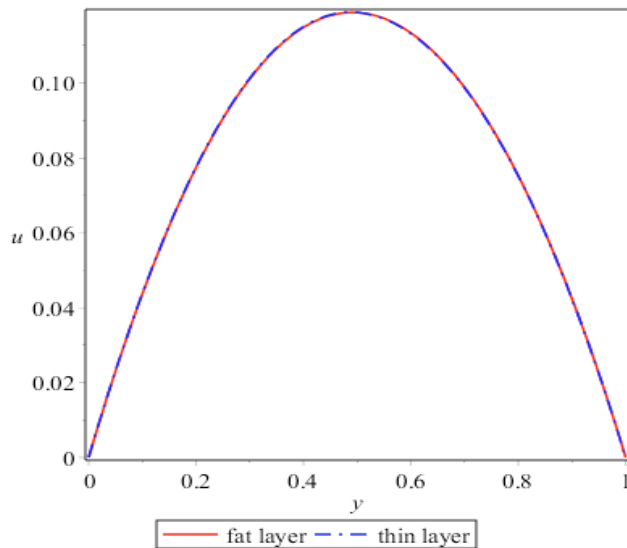


Figure 4: Velocity profile in the triple-layered configuration for thin and fat transition layers. $Da = 1$.

As Da decreases, the velocity profiles across the channel start deviating from the parabolic-like behavior

and the thin layer profiles velocity increases, as compared with the fat layer case. How the velocity profiles progress for decreasing Da is illustrated in Figures 5, 6, and 7, which show that the thin layer velocity becomes more pronounced, and increases relative to the fat transition layer profiles. This is the same behavior reported in [11], and may be interpreted in terms of the greater influence and higher momentum transfer the Navier-Stokes channel has on the thin transition layer for lower Da , thus increasing the velocity in the porous layers.

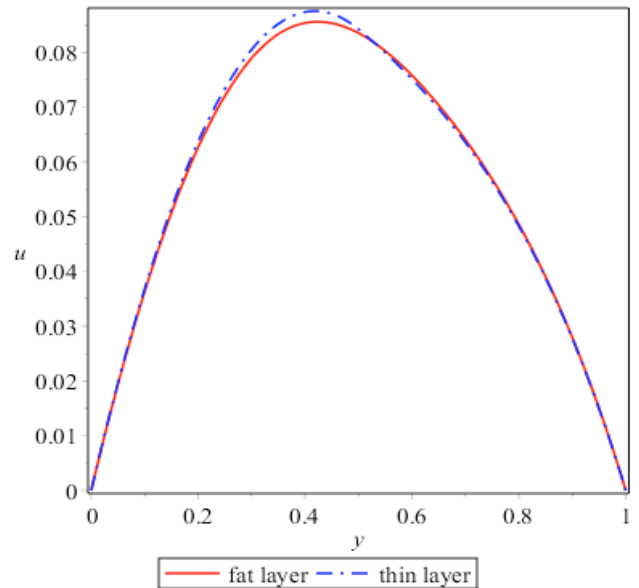


Figure 5: Velocity profile in the triple-layered configuration for thin and fat transition layers. $Da = 0.1$.

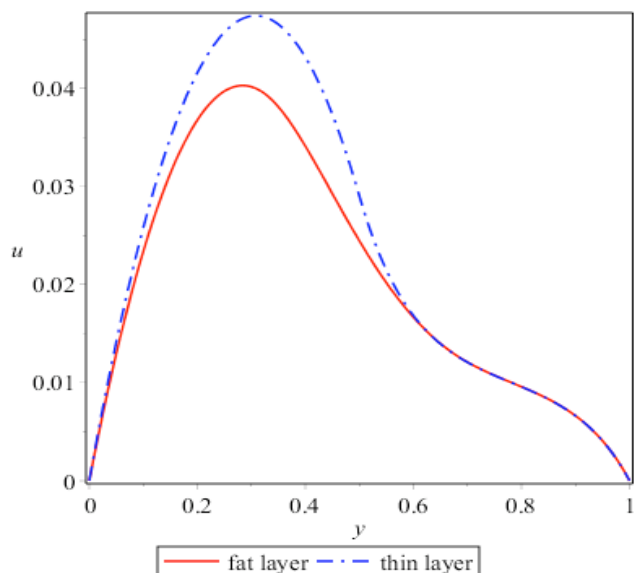


Figure 6: Velocity profile in the triple-layered configuration for thin and fat transition layers. $Da = 0.01$.

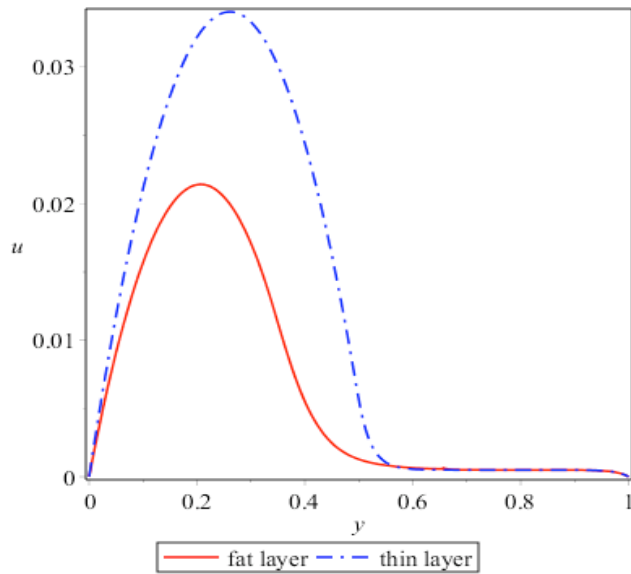


Figure 7: Velocity profile in the triple-layered configuration for thin and fat transition layers. $Da = 0.0005$.

The effects of changing Da on the velocity profiles for thin and fat layers are illustrated in Figures 8 and 9. In Figure 8, effects of Da are illustrated for the thick transition layer and show the increase in velocity with increasing Da . A similar behavior is illustrated for the thin layer, and shown in Figure 9. This expected behavior is interpreted to be due to the greater flow rate for larger Da , equivalently higher permeability.

CONCLUSION

In this work, ascending series expressions for the Nield-Koznetsov function were developed and

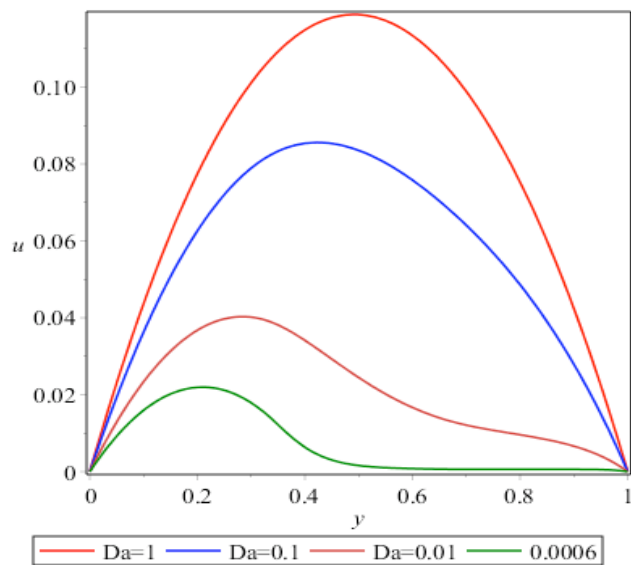


Figure 8: Velocity profile in the triple-layered configuration for a fat transition layer for different Da .

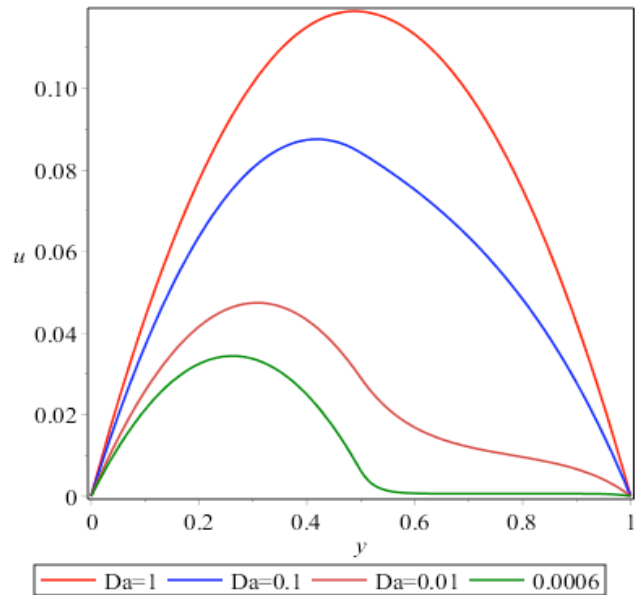


Figure 9: Velocity profile in the triple-layered configuration for a thin transition layer for different Da .

implemented in the study of the transition zone problem. The derived expressions produce highly accurate results, as has been discussed when an existing transition layer problem has been analyzed. Thin and fat transition layers have been considered and the velocity profiles show the increase in the thin layer velocity, relative to the thick layer, as a result of the greater momentum transfer from the channel to the fluid in the thin layer. The effects of increasing Darcy number on the velocity profile have been analyzed for thin and fat layers, and show the expected increase in the fluid velocity with increasing Darcy number. The flow through the channel over a Darcy layer has also been analyzed with the main conclusion that the mean Darcy velocity is a decreasing function of the slip parameter.

ACKNOWLEDGEMENTS

The authors would like to thank the referee for providing suggestions that enhanced this contribution.

The authors would also like to thank Dr. M.S. Abu Zaytoon for his assistance in the computations in this work.

S.M. Alzahrani wishes to acknowledge the support received from University of Umm Al-Qura, Kingdom of Saudi Arabia.

REFERENCES

- [1] Neale G and Nader W. Practical Significance of Brinkman's Extension of Darcy's law: Coupled Parallel Flows within a Channel and a Bounding Porous Medium. *Canadian J Chem Eng* 1974; 52: 475-478. <http://dx.doi.org/10.1002/cjce.5450520407>
- [2] Vafai K and Thiyagaraja R. Analysis of Flow and Heat Transfer at the Interface Region of a Porous Medium. *Int J Heat Mass Transfer* 1987; 30(7): 1391-1405. [http://dx.doi.org/10.1016/0017-9310\(87\)90171-2](http://dx.doi.org/10.1016/0017-9310(87)90171-2)
- [3] Vafai K and Kim SJ. Fluid Mechanics of the Interface Region between a Porous Medium and a Fluid Layer: An Exact Solution. *Int J Heat Fluid Flow* 1990; 11(3): 254-256. [http://dx.doi.org/10.1016/0142-727X\(90\)90045-D](http://dx.doi.org/10.1016/0142-727X(90)90045-D)
- [4] Alazmi B and Vafai K. Analysis of Variants within the Porous Media Transport Models. *Journal of Heat Transfer* 2000; 122: 303-326. <http://dx.doi.org/10.1115/1.521468>
- [5] Beavers GS and Joseph DD. Boundary Conditions at a Naturally Permeable Wall. *J Fluid Mech* 1967; 30(1): 197-207. <http://dx.doi.org/10.1017/S0022112067001375>
- [6] Sahraoui M and Kaviany M. Slip and No-slip Velocity Boundary Conditions at Interface of Porous, Plain Media. *Int J Heat Mass Transfer* 1992; 35: 927-943. [http://dx.doi.org/10.1016/0017-9310\(92\)90258-T](http://dx.doi.org/10.1016/0017-9310(92)90258-T)
- [7] Nield DA. The Boundary Correction for the Rayleigh-Darcy Problem: Limitations of the Brinkman Equation. *J Fluid Mech* 1983; 128: 37-46. <http://dx.doi.org/10.1017/S0022112083000361>
- [8] Chandesris M and Jamet D. Boundary Conditions at a Planar Fluid-Porous Interface for a Poiseuille Flow. *Int J Heat Mass Transfer* 2006; 49: 2137-2150. <http://dx.doi.org/10.1016/j.ijheatmasstransfer.2005.12.010>
- [9] Parvazinia M, Nassehi V, Wakeman RJ and Ghoreishy MHR. Finite Element Modelling of Flow through a Porous Medium between Two Parallel Plates Using the Brinkman Equation. *Transport in Porous Media* 2006; 63: 71-90. <http://dx.doi.org/10.1007/s11242-005-2721-2>
- [10] Abu Zaytoon MS. Flow Through and Over Porous Layers of Variable Thicknesses and Variable Permeability. PhD Thesis, University of New Brunswick, Saint John, Canada 2015.
- [11] Nield DA and Kuznetsov AV. The Effect of a Transition Layer between a Fluid and a Porous Medium: Shear Flow in a Channel. *Transport in Porous Media* 2009; 87: 477-487. <http://dx.doi.org/10.1007/s11242-009-9342-0>
- [12] Hamdan MH and Kamel MT. On the Ni(x) Integral Function and its Application to the Airy's Non-homogeneous Equation. *Applied Mathematics and Computation* 2011; 217: 7349-7360. <http://dx.doi.org/10.1016/j.amc.2011.02.025>

Received on 10-03-2016

Accepted on 06-04-2016

Published on 13-07-2016

DOI: <http://dx.doi.org/10.15377/2409-9848.2016.03.01.2>© 2016 Alzahrani *et al.*; Avanti Publishers.

This is an open access article licensed under the terms of the Creative Commons Attribution Non-Commercial License (<http://creativecommons.org/licenses/by-nc/3.0/>) which permits unrestricted, non-commercial use, distribution and reproduction in any medium, provided the work is properly cited.